Distinct Signaling Requirements for the Establishment of ESC Pluripotency in Late-Stage EpiSCs

Article

Cell Reports

Distinct Signaling Requirements for the Establishment of ESC Pluripotency in Late-Stage EpiSCs

Graphical Abstract

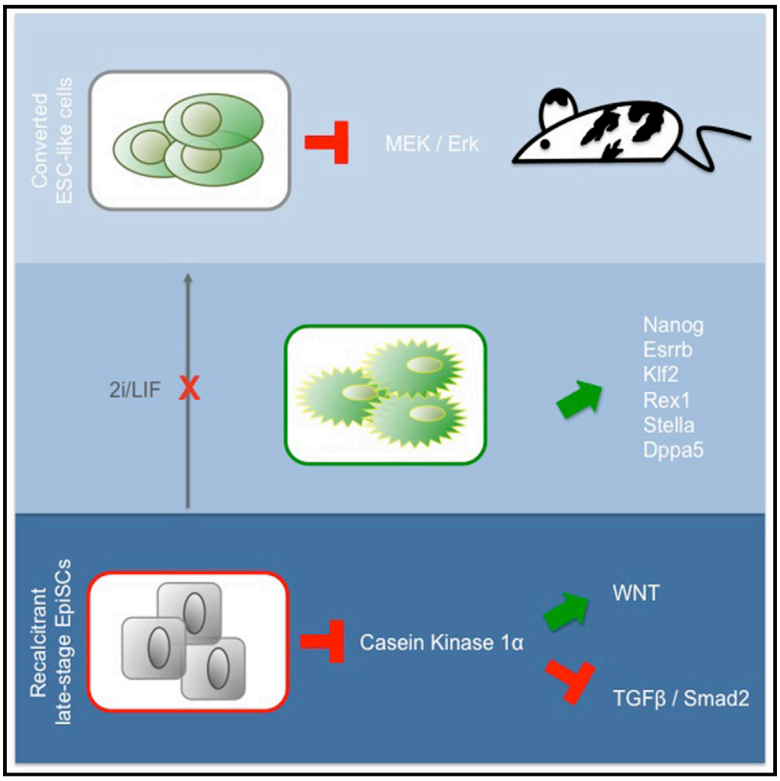

Authors

Damir Jacob Illich, Miao Zhang, Andrei Ursu, ..., Shaorong Gao, Herbert Waldmann, Hans R. Schöler

Correspondence

herbert.waldmann@mpi-dortmund.mpg.de (H.W.), office@mpi-muenster.mpg.de (H.R.S.)

In Brief

Illich et al. convert late-stage EpiSCs recalcitrant to the 2i/LIF method into germline-competent ESC-like cells through inhibition of casein kinase 1 alpha (CK1a) with the small molecule Epiblastin A. Inhibition of CK1a leads to WNT activation and TGFbeta/SMAD2 inhibition, which promotes the establishment and maintenance of the pluripotency network.

Highlights

- Inhibition of CK1alpha induces ESC conversion in EpiSCs recalcitrant to 2i/LIF
- The ESC conversion acts via WNT activation and TGFbeta/SMAD2 inhibition
- MEK inhibition stabilizes the conversion and restores germline competence
- CK1 inhibition promotes activation and maintenance of the pluripotency network

Illich et al., 2016, Cell Reports *15*, 787–800
April 26, 2016
http://dx.doi.org/10.1016/j.celrep.2016.03.073

CellPress

Cell Reports
Article

Distinct Signaling Requirements for the Establishment of ESC Pluripotency in Late-Stage EpiSCs

Damir Jacob Illich,[1,2,11] Miao Zhang,[1,11] Andrei Ursu,[2,4,11] Rodrigo Osorno,[1] Kee-Pyo Kim,[1] Juyong Yoon,[1] Marcos J. Araúzo-Bravo,[1,3,12] Guangming Wu,[1] Daniel Esch,[1] Davood Sabour,[1,13] Douglas Colby,[10] Kathrin S. Grassme,[5] Jiayu Chen,[6] Boris Greber,[7,8] Susanne Höing,[1] Wiebke Herzog,[1,5,9] Slava Ziegler,[2] Ian Chambers,[10] Shaorong Gao,[6] Herbert Waldmann,[2,4,*] and Hans R. Schöler[1,5,*]

[1]Max Planck Institute for Molecular Biomedicine, Röntgenstrasse 20, 48149 Münster, Germany
[2]Max Planck Institute for Molecular Physiology, Otto-Hahn-Strasse 11, 44227 Dortmund, Germany
[3]IKERBASQUE, Basque Foundation for Science, 48013 Bilbao, Spain
[4]Technische Universität Dortmund, 44227 Dortmund, Germany
[5]University of Münster, 48149 Münster, Germany
[6]School of Life Sciences and Technology, Tongji University, Shanghai 200092, China
[7]Human Stem Cell Pluripotency Laboratory, Max Planck Institute for Molecular Biomedicine, 48149 Münster, Germany
[8]Chemical Genomics Centre of the Max Planck Society, 44227 Dortmund, Germany
[9]Cells-in-Motion Cluster of Excellence (EXC 1003 - CiM), University of Münster, 48149 Münster, Germany
[10]MRC Centre for Regenerative Medicine, Institute for Stem Cell Research, School of Biological Sciences, University of Edinburgh, Edinburgh EH16 4UU, Scotland
[11]Co-first author
[12]Present address: Group of Computational Biology and Systems Biomedicine, Biodonostia Health Research Institute, 20014 San Sebastián, Spain
[13]Present address: Department of Genetics, Faculty of Medicine, Babol University of Medical Sciences, 47134 Babol, Iran
*Correspondence: herbert.waldmann@mpi-dortmund.mpg.de (H.W.), office@mpi-muenster.mpg.de (H.R.S.)
http://dx.doi.org/10.1016/j.celrep.2016.03.073

SUMMARY

It has previously been reported that mouse epiblast stem cell (EpiSC) lines comprise heterogeneous cell populations that are functionally equivalent to cells of either early- or late-stage postimplantation development. So far, the establishment of the embryonic stem cell (ESC) pluripotency gene regulatory network through the widely known chemical inhibition of MEK and GSK3beta has been impractical in late-stage EpiSCs. Here, we show that chemical inhibition of casein kinase 1alpha (CK1alpha) induces the conversion of recalcitrant late-stage EpiSCs into ESC pluripotency. CK1alpha inhibition directly results in the simultaneous activation of the WNT signaling pathway, together with inhibition of the TGFbeta/SMAD2 signaling pathway, mediating the rewiring of the gene regulatory network in favor of an ESC-like state. Our findings uncover a molecular mechanism that links CK1alpha to ESC pluripotency through the direct modulation of WNT and TGFbeta signaling.

INTRODUCTION

Pluripotency is defined as a cell's ability to differentiate into all somatic cell types. Two different pluripotent cell states have been proposed, which are commonly termed naïve and primed pluripotency. Mouse embryonic stem cells (ESCs) are derived from the inner cell mass (ICM) of developing embryos and have the ability to colonize preimplantation embryos after injection (Martin, 1981; Evans and Kaufman, 1981). This is a hallmark feature of naive pluripotency, but such pluripotency is not necessarily the first pluripotent state in development, as mouse ESCs correspond to day-4.5 and not day-3.5 ICMs (Boroviak et al., 2014). While scientists try to define the naive pluripotent state in humans (Dodsworth et al., 2015), it appears that the culture conditions of a pluripotent state corresponding to day-3.5 mouse embryos are yet to be defined.

In contrast to ESCs, epiblast stem cells (EpiSCs), which are derived from the epiblast of postimplantation embryos, can readily form teratomas and colonize embryos after being injected into the postimplantation epiblast (Huang et al., 2012). However, when cultured under standard conditions, EpiSCs rarely, if at all, contribute to embryo development after being injected into preimplantation embryos (Brons et al., 2007; Tesar et al., 2007; Han et al., 2010). These features are commonly considered to be the hallmark of primed pluripotency.

EpiSCs depend on basic fibroblast growth factor (bFGF) and Activin A signaling for maintaining pluripotency, while mouse ESCs require LIF together with inhibition of GSK3beta and fibroblast growth factor/extracellular-signal-regulated kinase (FGF/ERK). Mouse ESCs form small, compact, three-dimensional colonies, whereas EpiSCs grow as large, flat colonies. A small number of transcription factors that are highly expressed in ESCs, but not in EpiSCs, have been found to reprogram EpiSCs

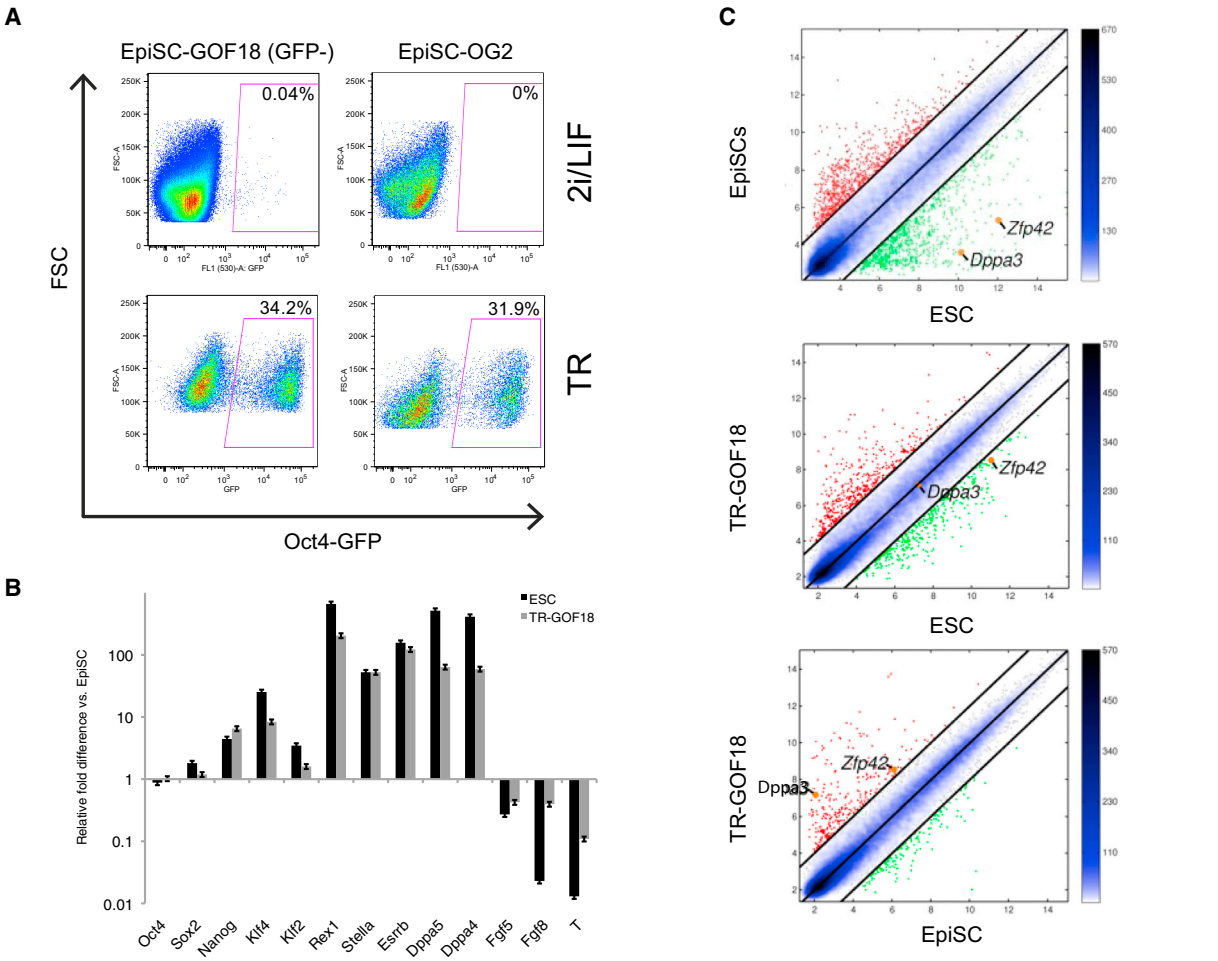

(legend on next page)

into ESCs (Tai and Ying, 2013; Gillich et al., 2012; Guo et al., 2009; Silva et al., 2009; Guo and Smith, 2010; Hall et al., 2009; Festuccia et al., 2012). Other studies have reported that the expression of transgenes is not required, and that EpiSCs could be converted into ESCs by a change in the culture conditions alone (Bao et al., 2009; Greber et al., 2010; Hanna et al., 2009; Chou et al., 2008; Ware et al., 2009).

The existence of at least one more distinct pluripotent state was previously revealed by our study, showing that EpiSC cultures display features of both early- and late-stage mouse epiblasts (Han et al., 2010). This work was prompted by the finding that EpiSCs display heterogeneity within a population (Tsakiridis et al., 2014; Han et al., 2010) and between different cell lines (Bernemann et al., 2011). Part of this heterogeneity is probably due to the broad developmental window of derivation. In this regard, it has been suggested that early-stage EpiSCs are susceptible to cellular reprogramming toward an ESC-like state, whereas late-stage EpiSCs are recalcitrant to this process (Han et al., 2010; Bernemann et al., 2011; Hayashi and Surani, 2009). However, the majority of EpiSCs functionally display features of late-stage postimplantation epiblasts.

Using a pteridine-derived inhibitor, which we discovered previously (Ursu et al., 2016), we here show that inhibition of casein kinase 1alpha (CK1alpha) can promote the efficient conversion of recalcitrant EpiSCs into ESC-like cells. Furthermore, we demonstrate that the conversion is mediated by the combined activation of WNT signaling and attenuation of transforming growth factor beta (TGFbeta) signaling, resulting in the activation of the ESC pluripotency gene regulatory network. These findings provide mechanistic insights into the molecular switch governing the transition between distinct pluripotent states.

RESULTS

Triamterene Induces Conversion of Late-Stage EpiSCs

Two Oct4 reporter lines (GOF18, which harbors all known Oct4 regulatory elements, and OG2, which lacks the proximal enhancer; PE) were used to study the different states of pluripotency (Yeom et al., 1996) (Figure 1A). ESCs of both reporter lines express GFP when cultured under ESC culture conditions (Bernemann et al., 2011; Han et al., 2010). The corresponding EpiSCs, when cultured under EpiSC conditions, do not express GFP, except for a small subpopulation previously shown to contribute to the formation of chimeras (Han et al., 2010). Both Oct4-GFP-negative GOF18 EpiSCs and OG2 EpiSCs were found to be recalcitrant to 2i/LIF-based ESC conversion, which is consistent with findings of previous reports (Bernemann et al., 2011; Han et al., 2010) (Figure 1A, upper).

In our initial screen, triamterene (TR) was identified using unsorted GOF18 EpiSCs. Here, we tested the effect of TR on the recalcitrant Oct4-GFP-negative fraction of the GOF18 EpiSC line, the EpiSC line OG2 (Figure 1), and the extremely recalcitrant cell lines T9 and C1a1 (Bernemann et al., 2011) (Figure S1). After culturing the Oct4-GFP-negative fraction with TR for 7 days, more than 30% were found to become GFP positive, even under EpiSC culture conditions (Figure 1A, bottom left). Similar results were obtained with the EpiSC line OG2 (Figure 1A, bottom right). In contrast, applying stringent mESC conditions alone (2i/LIF) failed to revert the different late-stage EpiSCs to a putative naive state (Figure 1A, upper).

Clonal lines from the TR-reverted GOF18 ESC-like cells (TR-GOF18) expressed ESC-specific markers, such as *Rex1*, *Stella*, *Klf2*, *Klf4*, and *Esrrb* (Figure 1B). In contrast, the expression of genes typically expressed in EpiSCs, such as *T-brachyury*, *Fgf5*, and *Fgf8*, was reduced in TR-induced cells. Most importantly, global gene expression analysis showed obvious assimilation of the gene expression profiles of TR-converted cells and ESCs (Figure 1C, middle; see also Figures 3A and S3B).

We then assessed the ability of TR to convert EpiSC lines (T9 and C1a1), which are especially resistant to media-induced conversion using 2i/LIF (Bernemann et al., 2011). We found that TR efficiently induces the reactivation of ESRRB and KLF4 proteins in T9 and C1a1 EpiSCs and promotes a change in colony morphology to small dome-shaped colonies (Figure 1D). The relative conversion efficiency of TR for these cell lines was measured based on the expression of the pluripotency marker *PECAM1*/CD31 (Figure S1A). After treatment with TR, the T9 and C1a1 cell lines expressed *PECAM1* at significantly lower levels than the other two cell lines (Figure S1A). The lower conversion rates of the T9 and C1a1 EpiSCs may partly be due to spontaneous differentiation even under EpiSC culture conditions (see differentiated areas in Figures 1D, S1B, and S3B for early differentiation markers, such as *Fgf5* and *Fgf8*).

Figure 1. TR Induces ESC Conversion of Recalcitrant EpiSCs

(A) Oct4-GFP expression after treatment with 2i/LIF (top) and TR (5 μM; bottom) for 7 days in sorted Oct4-GFP-negative GOF18 EpiSCs (left) and OG2 EpiSCs as measured by flow cytometry (FSC, forward scatter). The basal medium for the conversion with 2i/LIF was ESC medium (20% serum replacement in KO-DMEM) and, for the conversion with TR, EpiSC conditioned medium containing FGF2 and Activin A.

(B) Comparison of gene expression patterns in ESCs, TR-GOF18 cells, and EpiSCs. The expression levels are normalized to those of unsorted E3 EpiSCs (the data represent mean ± SD of triplicates; n = 3).

(C) Scatterplot of global gene expression microarrays comparing TR-GOF18 cells with ESCs (middle) and unsorted E3 EpiSCs (bottom). The comparison of unsorted E3 EpiSCs and ESCs (top) is shown as control. The black lines delineate the boundaries of 4-fold difference in gene expression levels. Genes highly expressed in TR-GOF18 cell samples compared with ESC samples are shown as red dots; those less expressed are shown as green dots. The positions of the pluripotent cell marker *Zfp42*/*Rex1* and the germ cell marker *Dppa3*/*Stella* are indicated as orange dots. The color bar to the right indicates the scattering density; the higher the scattering density, the darker the blue. The gene expression levels are depicted on $\log_2$ scale.

(D) Immunofluorescence analysis for Klf4 and Esrrb proteins in recalcitrant EpiSC lines C1a1 (top) and T9 (bottom) following treatment with TR for 7 days (the scale bar represents 200 μm).

(E) X chromosome reactivation and immunofluorescence analysis for Esrrb protein in female EpiSCs following treatment with TR for 7 days (the scale bar represents 200 μm).

See also Figure S1.

The effectiveness of TR in reinstating ESC pluripotency in EpiSCs was further tested using an X-Chromosome-GFP reporter in female EpiSCs (Hadjantonakis et al., 1998). This reporter had been previously shown to faithfully discriminate between ESCs and EpiSC-like cells, as this transgene specifically becomes reactivated in the naive state (Han et al., 2011).

The derivation of X-GFP EpiSCs has been previously described (Gillich et al., 2012). Hence, an induction of ESC pluripotency should lead to X chromosome reactivation, and, conversely, the expression of X-GFP would be indicative of a successful reversion of these cells. Culturing these EpiSCs in TR-containing media changed the morphology of these cells toward that of ESC-like colonies and, indeed, successfully promoted the reactivation of X-Chr-GFP and expression of ESRRB protein in these cells (Figure 1E).

During the conversion of GOF18 or OG2 EpiSCs with TR, the first dome-shaped Oct4-GFP-positive colonies appeared after 4 days. It was unclear whether TR was required throughout the whole culture period or whether a shorter exposure of TR would enable EpiSCs to convert under 2i/LIF conditions. To address this, sorted Oct4-GFP-negative E3 EpiSCs were treated with TR under EpiSC conditions for varying time periods, followed by further culturing under the 2i/LIF condition (Figure S1C). We found that pretreatment with TR even for 3 days followed by 2i/LIF did not produce any GFP-positive colonies. On the fourth day of TR treatment, the first Oct4-GFP-positive colonies appeared. However, even after 4 days, 2i/LIF did not have any effect on the number of colonies, as the medium lacking both TR and 2i/LIF gave the same number of colonies. We therefore concluded that TR had to be present for 6 days in order for EpiSCs to undergo efficient conversion to an ESC-like state (Figure S1C).

Taken together, the presence of TR during a period of 6 days induced the efficient conversion of late-stage EpiSCs toward a cellular state that is similar to that of ESCs.

PD0325901 Stabilizes the TR-Induced Transition to ESC Pluripotency

Although TR-converted cells and ESCs are quite similar, even clonal populations of E3 ESC-like cells always contained some Oct4-GFP-negative cells, which were not observed in ESCs cultured in KO-DMEM/KOSR (KO serum replacement)/LIF. We took this as an indication that TR on did not fully establish, and/or did not sufficiently maintain, ESC pluripotency (Figure 2A; compare left and middle). Analyses of gene expression and promoter methylation of ICM marker genes in these two TR-GOF18 populations showed that the Oct4-GFP-positive cell population more closely resembled ESC-like features than the Oct4-GFP-negative population. In fact, the latter cell fraction was more similar to EpiSCs (Figures S2A and S2B).

To achieve homogeneous and complete conversion of EpiSCs into ESC-like cells, we treated the TR-converted cells with a selected set of chemical inhibitors known to support ESC self-renewal, as well as with a collection of compounds synthesized in-house (Nie et al., 2012). We found that culturing the TR-converted cells in KO-DMEM/KOSR/LIF together with the MEK inhibitor PD0325901 (PD) dramatically increased the proportion of Oct4-GFP-positive cells after only 48 hr (Figure 2A; compare middle and right). TR/PD-converted cells and ESCs were indistinguishable with respect to cell morphology, growth characteristics, alkaline phosphatase (AP) activity, and Oct4-GFP expression (Figure S2C). At the molecular level, ESC-specific markers were (re-)expressed, while EpiSC markers were reduced in TR/PD-converted cells (Figure 2B). In contrast to EpiSCs, colonies of TR/PD-converted cells exhibited homogeneously expressed protein levels of SOX2, NANOG, and STELLA (Figure 2C).

ESCs preferentially use the distal enhancer (DE) to drive *Oct4* expression, while EpiSCs use the PE (Tesar et al., 2007; Yeom et al., 1996). Using a luciferase assay, we compared the activity of the *Oct4* enhancer in the reverted cells with that of ESCs and EpiSCs. The PE/DE ratio in TR/PD-reverted cells was tilted toward the preferential use of the *Oct4* DE, like ESCs but unlike EpiSCs (Figure 2D). In accordance, TR/PD cells exhibited a global gene expression pattern that closely resembled that of ESCs (Figure 2E; see also Figures 3A and S3B).

We next assessed the responsiveness of the TR/PD-reverted cells to ESC- and EpiSC-related signaling pathways (Figure S2D). In order to propagate, EpiSCs depend on TGFbeta/SMAD2/3 signaling, whereas ESCs require stimulation of the LIF/STAT3 pathway. Inhibition of LIF/STAT3 signaling in ESCs was found to induce differentiation, i.e., pluripotency markers were downregulated and early differentiation markers were upregulated, compared with the untreated control (Figure S2D, left; see ESC+JAKi). In contrast, inhibition of TGFbeta/SMAD2/3 signaling in EpiSCs induced differentiation (Figure S2D, right; see EpiSC+SB). Upon inhibition of these two pathways, TR/PD cells reacted, in both cases, similarly to ESCs and differently from EpiSCs, indicating a switch in the signaling pathways toward those related to ESC pluripotency (Figure S2D; see TR/PD+JAKi in left and TR/PD+SB in right). Notably, in both cases, TR-converted cells showed a more moderate response than ESCs and TR/PD-converted cells, again suggesting that TR alone primes EpiSCs for a complete switch of cell states (Figure S2D; see TR-GOF18+JAKi in left and TR-GOF18+SB in right).

Germline Competence Is Restored in TR/PD-Converted Cells

The converted cells were compared to EpiSCs and ESCs by global gene expression analysis. The heatmaps of TR/PD cells were found to be very similar to those of ESCs (Figure 3A), which was also confirmed by hierarchical clustering analysis (Figure S3A). The most differentially expressed genes between TR-converted and TR/PD cells give insight into the specific genetic changes that distinguish the two cell types (Figure S3B). For example, the ICM markers *Dppa5*, *Esrrb*, *Dppa4*, *Klf2*, and *Nr5a2* were expressed in TR-GOF18 cells at levels comparable to those in ESCs. Other ICM markers, such as *Tcl1*, *Tbx3*, and *Klf4*, were also strongly induced in TR-GOF18 cells compared with EpiSCs but reached the expression levels of ESCs only upon inhibition of the MEK pathway (addition of PD). MEK inhibition also resulted in the suppression of early differentiation markers, such as *Fgf5* and *Fgf8*, which were elevated in TR-GOF18 cells (or a subset thereof).

We then assessed whether the aforementioned switch in gene expression was accompanied by a global change in the methylation state of TR/PD-converted cells. Consistent with the gene expression data (Figures 1B and 2B), the endogenous

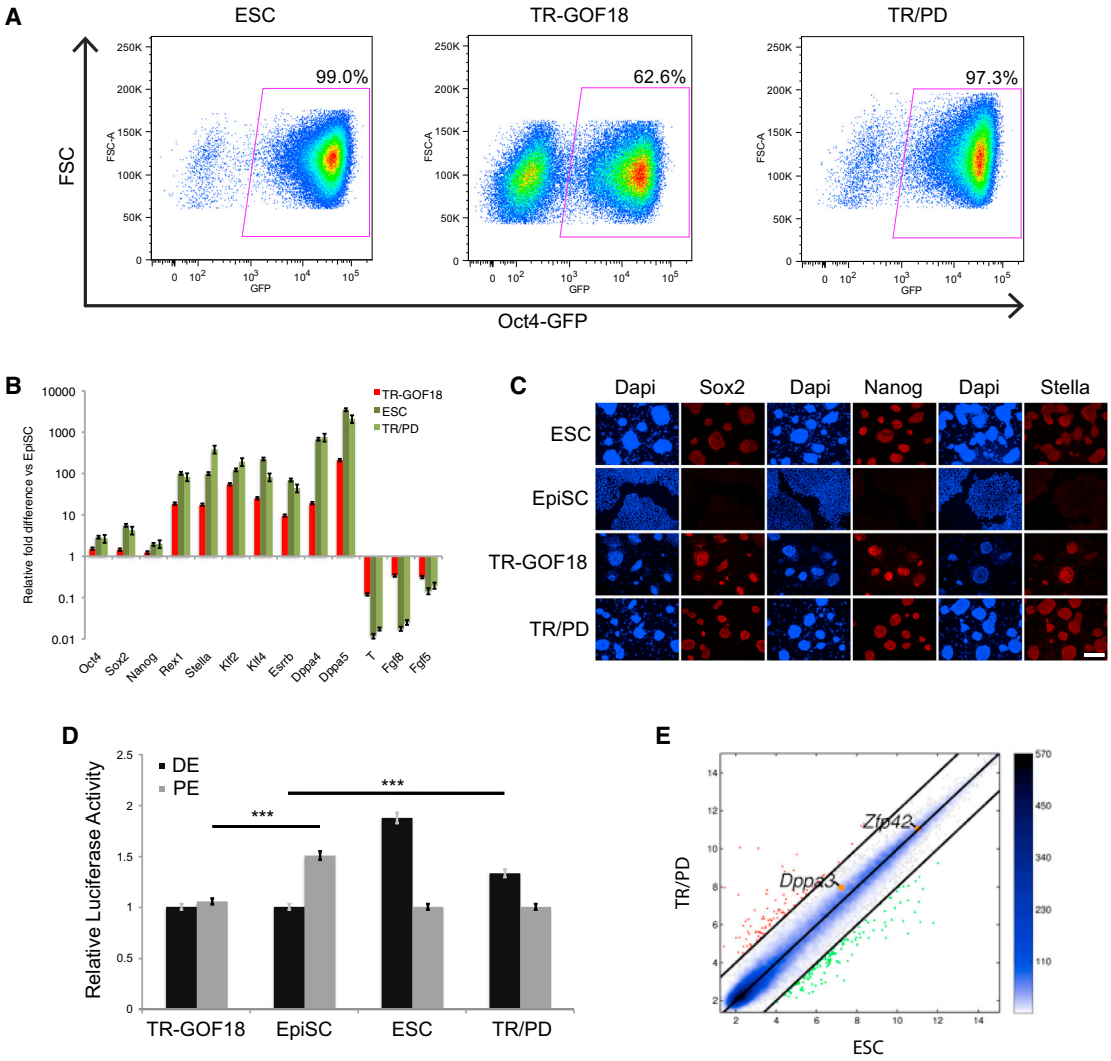

Figure 2. MEK Inhibition in TR-Treated Recalcitrant EpiSCs Improves the Transition to ESC Pluripotency

(A) Percentage of Oct4-GFP-positive cells in ESCs, TR-GOF18 cells, and TR/PD cells as measured by flow cytometry (forward scatter: FSC). TR-GOF18 represents a clonal cell line of TR-converted E3 EpiSCs, which was maintained under ESC culture conditions for more than 30 passages. The TR/PD represents a clonal cell line of TR-GOF18 cells after treatment with the MEK inhibitor PD (1 μM) for 2 days. The TR/PD cells were maintained under ESC culture conditions in the presence of PD.

(B) Comparison of gene expression patterns in ESCs, TR-GOF18 cells, and TR/PD cells. The expression levels are normalized to those of unsorted E3 EpiSCs (the data represent mean ± SD of triplicates; n = 3).

(C) Immunofluorescence analysis for Sox2, Nanog, and Stella (Dppa3) in ESCs, TR-GOF18 cells, EpiSCs, and TR/PD-converted cells. DAPI was used for nuclear staining (the scale bar represents 350 μm).

(D) Luciferase assay showing the ratios of Oct4 enhancer activity in ESCs, TR-GOF18 cells, EpiSCs, and TR/PD-converted cells. The enhancer activities in EpiSCs and TR-GOF18 cells are normalized to the DE activity, which is set to 1. The enhancer activities in ESCs and TR/PD cells are normalized to the PE activity, which is set to 1. The relative luciferase activities were also normalized to the activity of an empty vector (the data represent mean ± SD of triplicates; n = 3; and $p < 0.001$).

(E) Scatterplot of global gene expression microarrays comparing TR/PD cells with ESCs. For control scatterplots, see Figure 1C. The black lines delineate the boundaries of 4-fold difference in gene expression levels. The genes highly expressed in TR/PD samples compared with ESC samples are shown as red dots; those less expressed are shown as green dots. The positions of the pluripotent cell marker *Zfp42*/*Rex1* and the germ cell marker *Dppa3*/*Stella* are indicated as orange dots. The color bar to the right indicates the scattering density; the higher the scattering density, the darker the blue color. The gene expression levels are depicted on $\log_2$ scale.

See also Figure S2.

Oct4 promoter was found to be completely unmethylated in both ESCs and EpiSCs, while the Oct4-GFP transgene promoter was mainly unmethylated in ESCs and highly methylated in EpiSCs (Figure 3B). In TR/PD cells, the Oct4-GFP transgene promoter was basically unmethylated, whereas in TR-converted cells, the transgene promoter was only partially unmethylated.

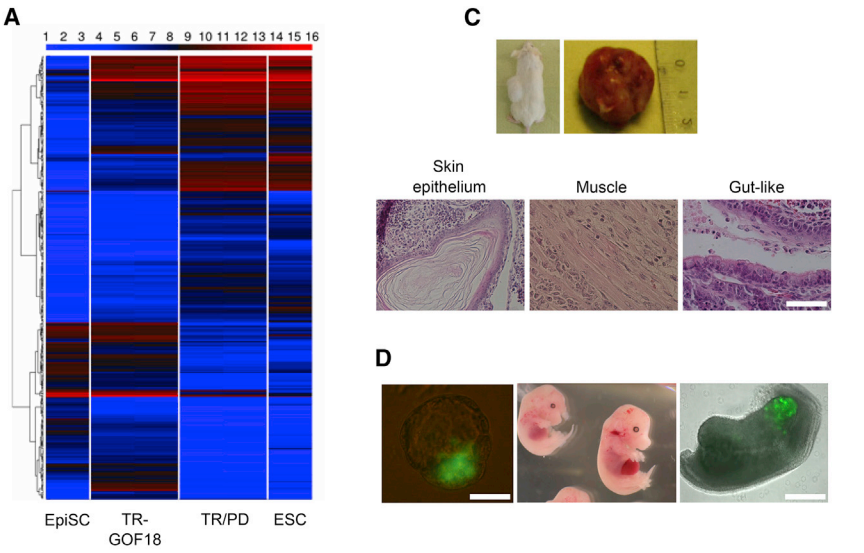

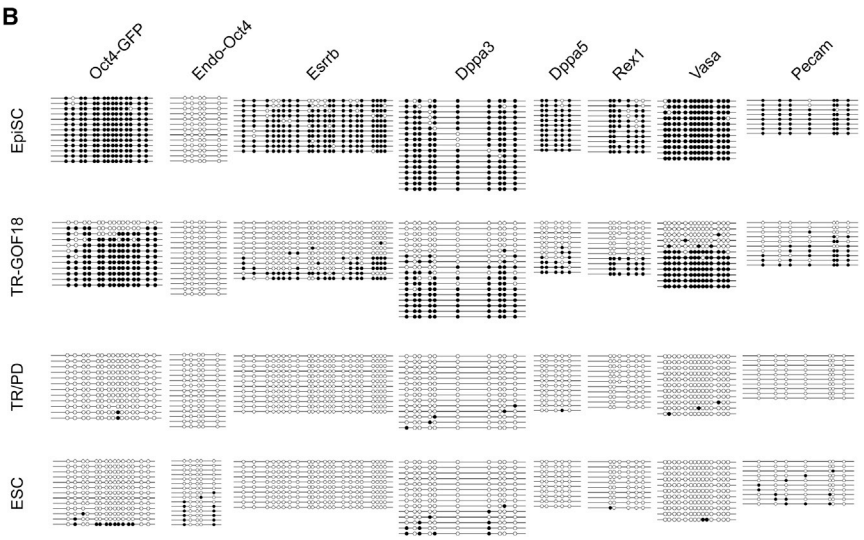

Figure 3. Combined Treatment with a MEK Inhibitor and TR Restores Germline Competency in EpiSCs

(A) Heatmap of global gene expression patterns in ESCs, TR-GOF18 cells, unsorted E3 EpiSCs, and TR/PD cells. The color bar at the top codifies the gene expression in $\log_2$ scale. The red and blue colors indicate high and low gene expression levels, respectively.

(B) DNA methylation status of the promoter regions of ICM marker genes in ESCs, TR-GOF18 cells, unsorted E3 EpiSCs, and TR/PD cells was analyzed using bisulfite-sequencing PCR.

(C) Representative image of a teratoma derived from TR/PD cells in a teratocarcinoma assay, together with representative tissues of ectodermal (skin epithelium), mesodermal (muscle), and endodermal (gut-like) lineages in teratomas obtained from TR/PD cells (the scale bar represents 50 μm).

(D) Embryonic and germline contribution of TR/PD cells. The blastocyst injection using TR/PD cells was performed, and the contribution of the cells to the ICM (left; the scale bar represents 50 μm), midterm (E14.5) pups (middle), and germline (right; the scale bar represents 450 μm) was assessed. See also Figure S3.

Demethylation was also observed for other marker genes analyzed in TR/PD-converted cells (Figure 3B).

Following global gene expression and methylation analysis, we sought to functionally characterize the reverted cells using in vivo differentiation assays. TR/PD-converted cells were found to give rise to teratomas containing tissues of all germ layers (Figure 3C). Most importantly, upon injection into blastocysts, TR/PD-converted cells showed successful integration into the ICM and, consequently, contribution to the germline (Figure 3D).

The TR Derivative Epiblastin A Is a Potent Inducer of ESC Pluripotency in EpiSCs

Kinase profiling and subsequent gene knockdown (KD) experiments had revealed that CK1alpha is a target enzyme in TR-induced ESC conversion, and structure-activity relationship analyses with chemically synthesized derivatives of TR yielded Epiblastin A as the most potent TR-derived CK1 inhibitor (Ursu et al., 2016).

Next, the ability of Epiblastin A to promote the reversion of EpiSCs was analyzed in further detail. Among the set of compounds examined, Epiblastin A was found to exhibit the highest conversion efficiency based on Oct4-GFP and *PECAM1* reactivation, almost 2-fold higher than TR (Figure 4A). CH and sodium butyrate had a negligible effect on the reactivation of Oct4-GFP and *PECAM1* (Figure 4A). This is a compelling finding, as Epiblastin-A-converted cells exhibited similar cell morphology; Oct4-GFP expression; AP immunoreactivity; protein levels of SOX2, NANOG, and STELLA; and gene expression profiles as ESCs (Figures 4B–4D). Most importantly, Epiblastin A/PD-converted cells regained the ability to contribute to chimera development when injected into blastocysts (Figure 4E).

CK1 Inhibition Promotes the Activation/Maintenance of the ESC Pluripotency Gene Regulatory Network

The next question was how the inhibition of CK1 influenced the expression of known pluripotency factors. To address this point, EpiSCs were treated with TR for 2, 4, 6, and 8 days. Notably, the expression of *Klf2*, *Nanog*, and *Esrrb* was upregulated from day 2 onward, albeit with different dynamics (Figure 5A). After 8 days of treatment with TR, expression levels of *Nanog* and *Esrrb* even exceeded those in ESCs. This result was recapitulated using D4476, an independent inhibitor of CK1 (Figure S4A).

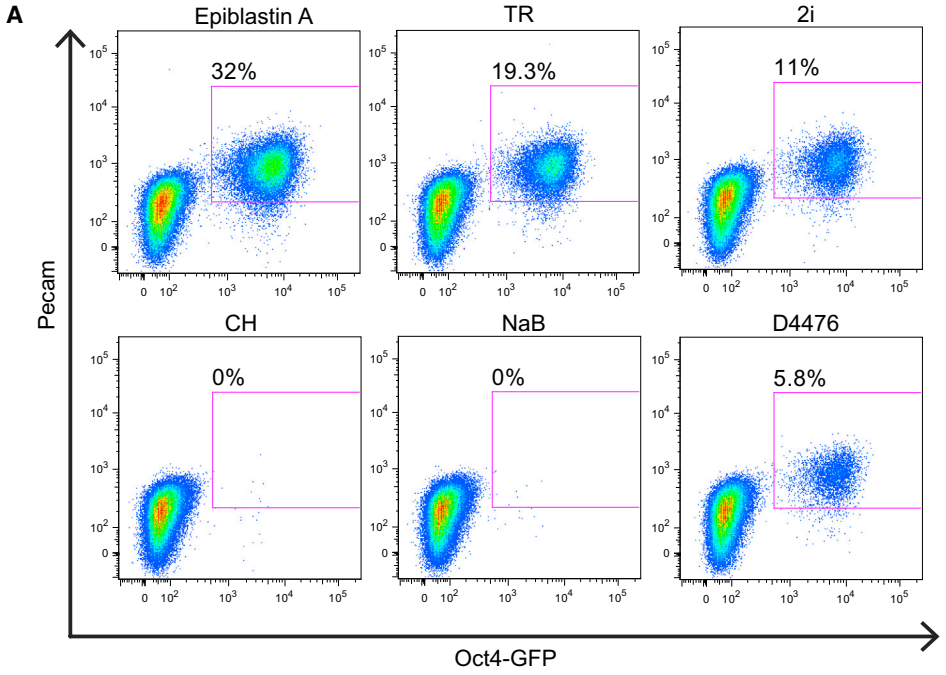

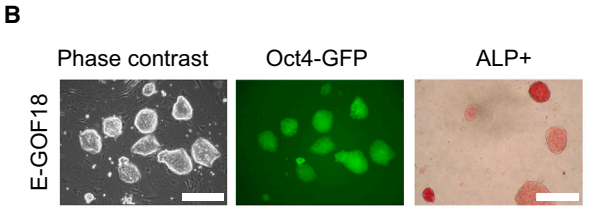

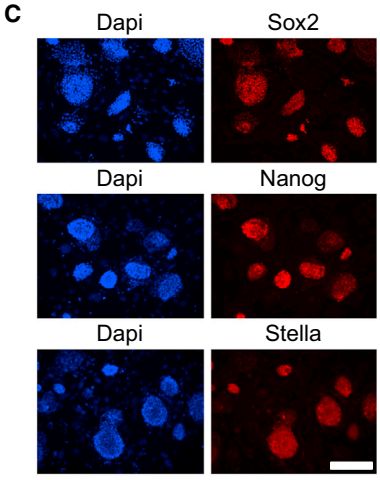

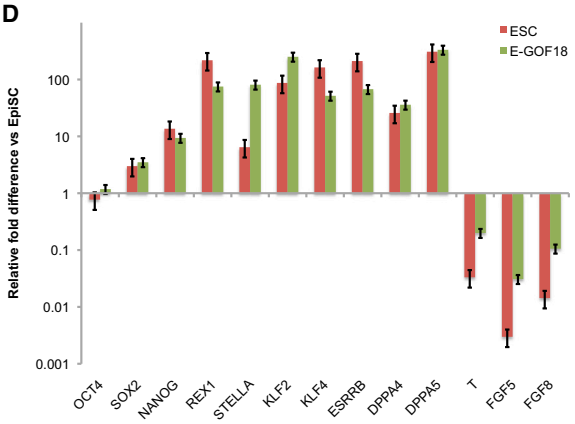

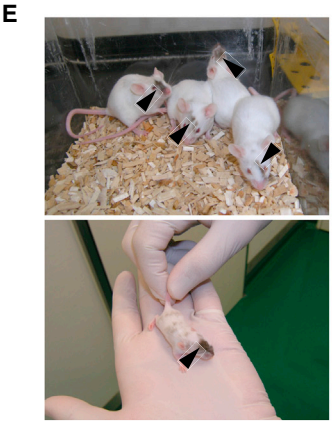

(legend on next page)

Next, the role of *Klf2*, *Nanog*, and *Esrrb* during Epiblastin-A-based conversion was determined by small hairpin RNA (shRNA)-based KD experiments (Figures 5B and S4B). *Nanog* KD, by far, had the strongest effect, as it essentially abolished reversion by Epiblastin A. *Klf2* KD also significantly reduced reversion efficiencies, suggesting critical roles for both Nanog and Klf2 in the process of reprogramming. *Esrrb* KD had a less dramatic effect, reducing the action of Epiblastin A by about 30% (Figure 5B).

As CK1 inhibitors have an impact on key pluripotency genes during the reversion of EpiSCs into ESC-like cells, we sought to test whether Epiblastin A and TR can affect self-renewal based on their ability to maintain the pluripotency gene regulatory network. High levels (5 μM and above) of Epiblastin A or TR were found to be toxic (data not shown), and N2B27 medium alone was not permissive for ESC self-renewal. However, following a titration experiment, an optimal working concentration of 2 μM Epiblastin A was found to promote clonal expansion of ESCs in N2B27. Addition of either LIF or PD to Epiblastin-A-supplemented media increased the cells' ability to self-renew, whereas addition of CH to Epiblastin-A-supplemented media decreased their ability (Figure 5D).

Upon switching to EpiSC media (based on N2B27/Activin A/bFGF), ESCs acquire properties of primed pluripotency (Guo et al., 2009). Nanog-GFP ESCs show progressive downregulation of Nanog-GFP under this condition (Chambers et al., 2007; Karwacki-Neisius et al., 2013). WNT signaling has been reported to prevent the commitment of ESCs into EpiSCs (ten Berge et al., 2011). Consistent with this observation, we found that downregulation of Nanog-GFP during EpiSC differentiation was blocked by the addition of TR, with an efficacy comparable to that of the WNT agonist CH (Figure 5C). On the other hand, ESCs cultured in the presence of serum and LIF are known to exhibit transcription factor heterogeneity, coinciding with the presence of cells with different self-renewal abilities (Chambers et al., 2007). To test the ability of TR to maintain the homogeneous expression of ICM transcription factors, we used the two reporter lines Nanog-GFP and Esrrb-Tomato. TR treatment induced a high and homogeneous expression of Nanog-GFP and Esrrb-Tomato for the duration of the assay, whereas untreated controls gave rise to Nanog-GFP-negative and Esrrb-Tomato-negative cells (Figure S4C).

Inhibition of CK1alpha Results in Simultaneous Activation of WNT Signaling and Inhibition of TGFbeta/SMAD2 Signaling

We next turned our attention to the mechanism underlying the inhibition of CK1. Signaling pathways known to be involved in ESC pluripotency were analyzed by using CK1 inhibitors. We found that Epiblastin A prevented phosphorylation of BCATENIN and SMAD2 (Figure 6A). It also affected STAT3 phosphorylation, probably due to inhibition of PI3K, as identified by kinase profiling. In contrast, ERK (and, consequently, probably the entire ERK pathway) was not affected (Figure 6A).

Following the inhibition of phosphorylation of BCATENIN, we further analyzed the effect of Epiblastin A and TR on the WNT pathway. To determine the enrichment of factors associated with signaling pathways, a Gene Ontology enrichment analysis was performed with the genes that were significantly upregulated within 12 hr of treatment of EpiSCs with TR. Based on this analysis, the WNT receptor signaling pathway clearly ranked at the top of significantly enriched "biological process" terms (Figure S5A). The known WNT/TCF (T-cell-factor) target genes *Axin2*, *Cdx1*, and *T-brachyury* were upregulated upon TR treatment (Figure S5B) (Kelly et al., 2011). We then performed the TOPFlash TCF-Luciferase assay to assess the WNT-inducing activity of Epiblastin A and found that Epiblastin A was more active than CH (Figure 6B).

Then we tested whether the positive effect of Epiblastin A treatment on ESC self-renewal was dependent on the WNT/BCATENIN pathway (Figure 5D). To this end, we used an ESC line in which both BCATENIN alleles had been floxed and that carried a CreERT2 cassette inserted into the ROSA26 locus (BCATENIN$^{fl/fl}$) (Brault et al., 2001; Tsakiridis et al., 2014). Treatment of BCATENIN$^{fl/fl}$ ESCs with 4-hydroxytamoxifen induced the deletion of both BCATENIN alleles, generating BCATENIN$^{-/-}$ ESCs (Figure 6D, western blot). BCATENIN$^{-/-}$ ESCs were unable to self-renew in the presence of CH/PD (2i) or CH/LIF (Figure 6D, right). The combined presence of only PD and LIF supports self-renewal in the absence of BCATENIN, albeit with decreased efficiency (Wray et al., 2011). Interestingly, although self-renewal efficiency was equally diminished by the depletion of BCATENIN, Epiblastin A was still capable of sustaining the ESC state (Figure 6D, right).

Finally, we assessed the potential of Epiblastin A and TR to modulate the WNT pathway in vivo. Zebrafish embryos 7–48 hr postfertilization (hpf) were kept in the presence of Epiblastin A or TR. At 48 hpf, zebrafish embryos exhibited a phenotype characteristic of WNT overactivation during this period of development, including impaired development of the eyes, forehead, and tail (Figure 6C).

P-SMAD2 was affected by both Epiblastin A and TR (Figure 6A). Therefore, we determined the role of SMAD2 during the reversion process. We hypothesized that Epiblastin A and TR might act by inhibiting the phosphorylation of both BCATENIN and SMAD2; therefore, we simulated this action by using CH together with

Figure 4. The TR Derivative Epiblastin A Is a Potent Inducer of ESC Pluripotency in EpiSCs

(A) Percentage of Oct4-GFP and *PECAM1* (*CD31*) double-positive cells after 7 days of ESC conversion with Epiblastin A (5 μM), TR (5 μM), 2i (PD: 1 μM and CH: 3 μM), CH (3 μM), NaB (100 μM), and D4476 (20 μM) in unsorted GOF18 EpiSCs as measured by flow cytometry.

(B) Morphology, Oct4-GFP, and ALP expression in Epiblastin A-GOF18 cells (left; the scale bars represent 300 μm).

(C) Immunofluorescence analysis for Sox2, Nanog, and Stella (Dppa3) in Epiblastin A-GOF18 cells. DAPI was used for nuclear staining (right; the scale bar represents 300 μm).

(D) Comparison of gene expression patterns in ESCs, Epiblastin A-GOF18 cells, and EpiSCs. The expression levels are normalized to those of EpiSCs (the data represent mean ± SD of triplicates; n = 3).

(E) Chimeric mice derived from Epiblastin A-GOF18 cells after blastocyst injection.

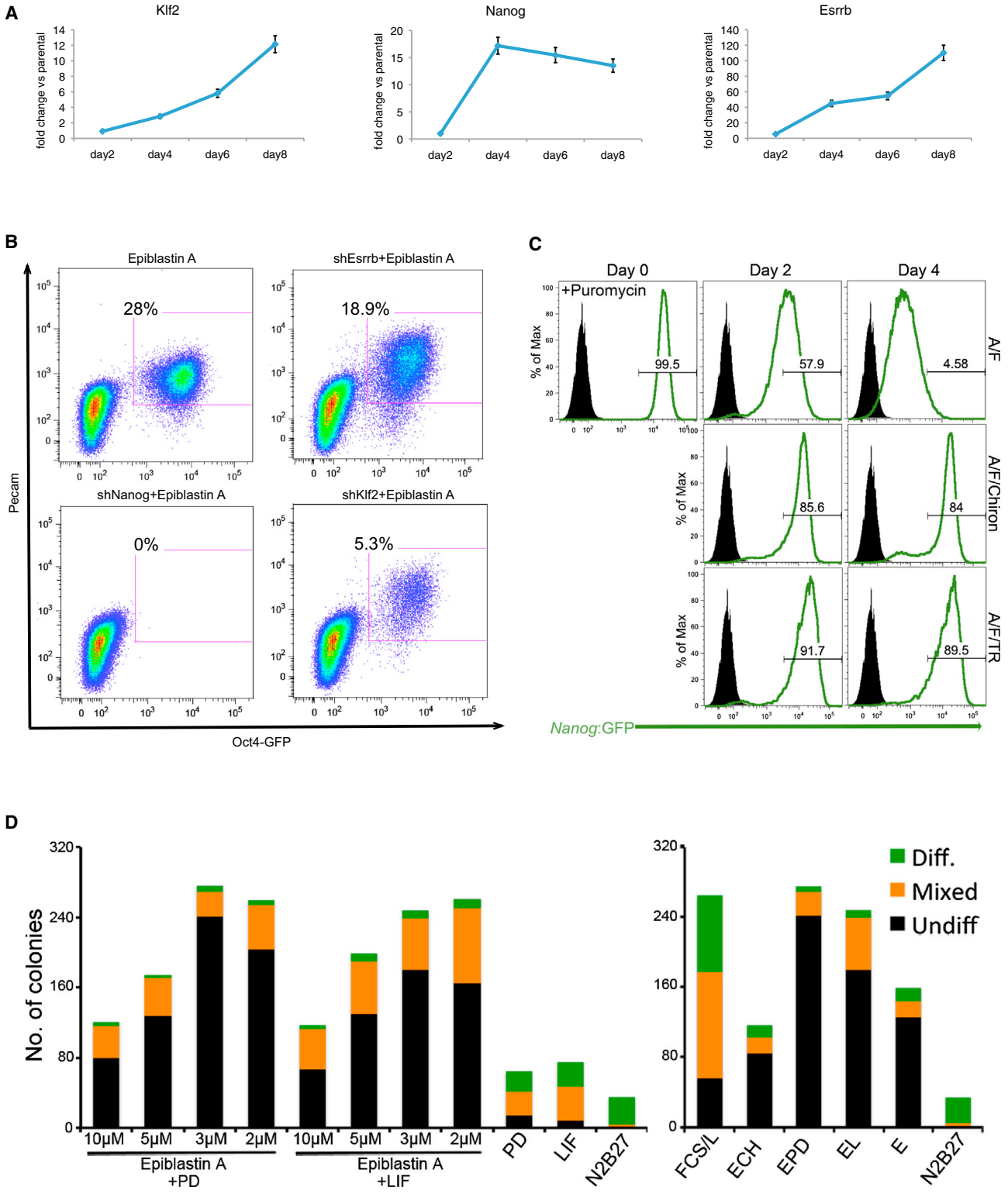

Figure 5. Casein Kinase 1 Inhibition Promotes the Activation/Maintenance of the ESC Pluripotency Gene Network

(A) Time-course analysis for whole mRNA expression of *Klf2*, *Nanog*, and *Esrrb* in TR-treated EpiSCs. The gene expression levels are normalized to those of untreated EpiSC samples (the data represent mean ± SD of triplicates; n = 3).

(B) Percentage of Oct4-GFP and *PECAM1* (*CD31*) double-positive cells after 6 days treatment with Epiblastin A, together with shRNA-based KD of *Esrrb*, *Nanog*, and *Klf2*, respectively, in GOF18 EpiSCs as measured by flow cytometry.

(legend continued on next page)

SB431542 (SB), an inhibitor of TGFbeta/SMAD2/3 signaling. Interestingly, while CH or SB promoted the differentiation of EpiSCs, when combined, they gave rise to ESC-like colonies expressing Oct4-GFP and ICM marker genes at levels comparable to those of ESCs (Figures 6E and 6F). Just like with Epiblastin A or TR, the conversion with CH/SB took 4–6 days and could even be achieved under EpiSC culture conditions.

A role for different CK1 isoenzymes in BCATENIN and SMAD2 phosphorylation had been reported by earlier studies (Amit et al., 2002; Waddell et al., 2004). We had previously found that KD of CK1alpha gave rise to a significant percentage of Oct4-GFP-positive cells compared with KD of either CK1epsilon or CK1delta. To determine whether a particular CK1 isoenzyme is involved in BCATENIN and SMAD2 phosphorylation, we performed an shRNA (short-hairpin-RNA)-based KD of CK1alpha, CK1delta, and CK1epsilon in EpiSCs (Figure S5C). Western blot analysis revealed that KD of either CK1alpha or CK1epsilon affected the phosphorylation of both BCATENIN and SMAD2 (Figure S5D). As TR did not inhibit GSK3beta and ALK (Ursu et al., 2016), these findings suggest that Epiblastin A and TR act on BCATENIN and SMAD2 phosphorylation via CK1alpha and CK1epsilon. Having obtained a significant population of Oct4-GFP-positive cells after KD of CK1alpha in E3 EpiSCs, we then derived and stably maintained a clonal cell line from this population. These cells strongly resembled ESCs in morphology, growth behavior, and Oct4-GFP expression. Global gene expression profiling revealed a gene expression pattern indistinguishable from that of ESCs (Figure S5E).

Finally, we sought to clarify the role played by LIF in the reversion process. TR was found to inhibit PI3K, which may explain the blocked STAT3 phosphorylation, pointing toward a redundancy of this pathway during conversion (Figure 6A). Moreover, ESCs could be maintained with Epiblastin A alone, i.e., without LIF (Figure 5D), and SB/CH could equally maintain ESCs without LIF (data not shown). To categorically determine whether LIF/STAT3 signaling is involved in Epiblastin-A-mediated self-renewal, we used *Stat3*$^{-/-}$ ESCs. These ESCs require CH/PD (2i) supplementation for propagation (Ying et al., 2008). In the absence of *Stat3*, Epiblastin-A-mediated self-renewal was severely reduced in the presence of either LIF or CH (Figure S5F). In contrast, the dual inhibition of ERK and CK1 (N2B27/PD/Epiblastin A) promoted the robust propagation of *Stat3*$^{-/-}$ ESCs, for more than 2 months (Figure S5F). *Stat3*$^{-/-}$ ESCs cultured for more than 2 months in PD/Epiblastin A were found to retain robust expression of OCT4, NANOG, ESRRB, and KLF4 proteins and to give rise to chimeric mice after blastocyst injection (Figures S5G and S5H). Taken together, our data suggest a concise mechanism of action for Epiblastin A and TR that is based on BCATENIN and SMAD2 modulation via inhibition of CK1alpha (Figure 6G).

DISCUSSION

As previously shown, EpiSCs are heterogeneous within and among cell lines (Bernemann et al., 2011; Han et al., 2010; Tsakiridis et al., 2014; Bao et al., 2009). Only a small subpopulation of EpiSCs displays features of the early postimplantation epiblast (Bao et al., 2009; Han et al., 2010), whereas the vast majority of EpiSCs functionally represent cells of late-stage postimplantation epiblast. Early-stage EpiSCs are susceptible to media-induced reversion into cells of an ESC-like state, whereas late-stage EpiSCs are refractory to this process (Figure 1A) (Bernemann et al., 2011; Han et al., 2010). In this study, we show that a small molecule compound, which was previously discovered in our laboratory, is capable of inducing the reversion of both early- and late-stage EpiSCs into ESC-like cells, and we herein describe its underlying mechanism of action. To our knowledge, this is the first study showing the robust conversion of late-stage EpiSCs into ESCs through chemical means only.

The conversion of EpiSCs into ESC-like cells by Epiblastin A and TR displays several striking features. After a relatively short exposure period to induce ESC pluripotency (6–8 days), cells converted by Epiblastin A or TR could be clonally expanded and maintained in LIF-supplemented ESC medium, without needing to further add either inhibitor. Notably, we found that TR induces the expression of Oct4-GFP in EpiSC medium in the absence of exogenous LIF. This likely occurs due to the presence of LIF in MEF (mouse embryonic fibroblast)-conditioned medium. However, Epiblastin A and TR were also found to inhibit PI3K-mediated STAT3 phosphorylation, indicating a redundancy of this pathway during the conversion process (Figure 6A).

Activation of the FGF/ERK pathway predisposes ESCs to differentiation (Greber et al., 2010; Kunath et al., 2007). Conversely, ERK inhibition, in combination with LIF and/or CH, supports the maintenance of undifferentiated ESCs (Ying et al., 2008). This is consistent with our observation that ERK inhibition in TR-converted cells finalizes and/or stabilizes the transition of these cells to ESC pluripotency (Figures 2 and 3).

Several kinase inhibitors have been reported either to support the generation of induced pluripotent stem (iPS) cells or to promote the conversion to ESC-like pluripotency (Ying et al., 2008; Li and Rana, 2012; Sato et al., 2004; Ichida et al., 2009; Maherali and Hochedlinger, 2009). Notably, TR did not inhibit GSK3beta, MEK/ERK, or ALK4/5, which are all targets of inhibitors that promote the reversion of EpiSCs into ESC-like cells (Greber et al., 2010; Zhou et al., 2010). This observation suggested that TR must be working through the regulation of a different kinase.

Kinase profiling revealed that Epiblastin A and TR inhibited CK1 isoenzymes, and KD of CK1alpha gave rise to Oct4-GFP-positive colonies; inhibiting either CK1epsilon or CK1delta had no effect at all. These cells had a gene expression profile that

(C) Differentiation of ESCs into EpiSCs is blocked by supplementation with TR. The flow-cytometry analysis of *Nanog*-GFP-positive cells during EpiSC differentiation (A/F) and in the presence of either Chiron or TR is shown (A, Activin A; F, bFGF). Black cell population represents non-fluorescent control cells). Puromycin selects for the expression of Nanog. The selection cassettes are part of the reporter construct that was knocked in into the Nanog locus.
(D) Clonal assay of ESCs in the indicated culture conditions. The ESCs were plated onto gelatin-coated plates and cultured for 7 days, after which, the cells were stained for AP and counted (L, LIF; E, Epiblastin A).
See also Figure S4.

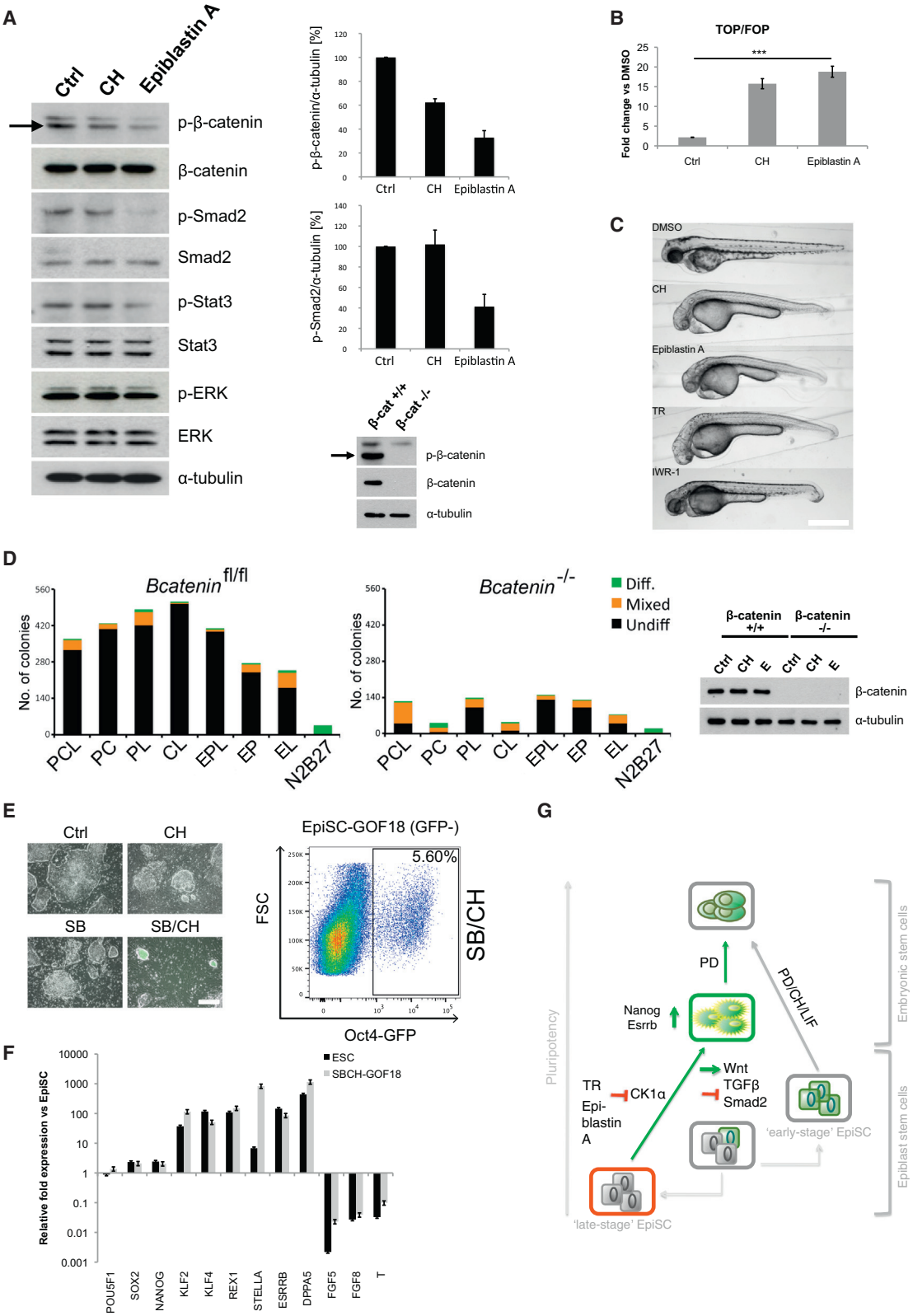

(legend on next page)

was indistinguishable from that of ESCs, and KD of CK1alpha resulted in reduced BCATENIN and SMAD2 phosphorylation, thus further substantiating a role for CK1alpha in the reprogramming process (Figures S5C and S5D).

CK1 family members are known to exert both negative and positive effects on WNT signaling (Price, 2006). Potential contact points for negative WNT regulation via CK1-mediated phosphorylation include BCATENIN (Amit et al., 2002; Liu et al., 2002), APC (Rubinfeld et al., 2001), and LRP5/6 (Swiatek et al., 2006). However, members of the CK1 family are also known to be involved in numerous other processes, including p53 and E-cadherin modifications, nuclear-cytoplasmic shuttling of transcription factors, and TGFbeta signaling (Rena et al., 2004; Waddell et al., 2004; Knippschild et al., 1997; Dupre-Crochet et al., 2007). It is also known that TR inhibits dihydrofolate reductase, acting as an antifolate due to the common pteridine structure of these two proteins (Corcino et al., 1970; Schalhorn et al., 1981). The resulting inhibition of DNA synthesis could explain the toxicity of Epiblastin A and TR when used in higher concentrations.

We confirmed the agonistic effect of Epiblastin A and TR on the WNT pathway both in vitro and in vivo. Furthermore, we showed that both Epiblastin A and TR simultaneously modulate WNT/BCATENIN and TGFbeta/SMAD2 signaling by inhibiting CK1alpha. Accordingly, we could also demonstrate that simultaneous activation of the WNT pathway and inhibition of SMAD2 signaling can mimic the Epiblastin-A- or TR-based reprogramming mechanism, in contrast to perturbing the two pathways individually (Figures 6 and S5). That is why neither SB nor CH could convert EpiSCs to ESC pluripotency.

Treatment of EpiSCs with TR coincided with strong upregulation of the key ESC-specific pluripotency markers *Klf2*, *Nanog*, and *Esrrb* (Figure 5A). Interestingly, KD of *Klf2* or *Nanog* significantly impaired Epiblastin-A/TR-based EpiSC reversion, highlighting the importance of these factors during this process (Figure 5B). KD of *Esrrb* reduced the number of Epiblastin-A-induced Oct4-GFP-positive cells by half (Figure 5B). However, shRNA probes for *Esrrb* were less efficient than those for *Nanog* and *Klf2* (Figure S4B). These intrinsic factors may be important for the chemical-induced reversion of EpiSCs, consistent with previous reports that they are efficient in promoting conversion when expressed ectopically (Festuccia et al., 2012; Silva et al., 2009; Hall et al., 2009).

Taken together, our results demonstrate not only that ESC pluripotency can be induced in late-stage EpiSCs, but also that this conversion can be made simple and very efficient. Moreover, our findings reveal insights into the mechanisms governing the transition between distinct states of pluripotency. This is of special interest, as we describe the conversion of the two extremes of pluripotency that have been defined to date. Notably, we introduce CK1alpha as a key player in the regulation of ESC pluripotency, through the direct modulation of WNT/BCATENIN and TGFbeta/SMAD2 signaling. These findings open the door to addressing numerous questions. For example, we can now determine whether the role of CK1 in the regulation of ESC pluripotency is conserved across species. Additionally, by means of CK1 inhibition and appropriate culture conditions, we now can define a pluripotent state that corresponds to day 3.5 ICMs.

EXPERIMENTAL PROCEDURES

Cell Culture

The derivation of EpiSC lines is described elsewhere (Greber et al., 2010). EpiSCs were cultured on feeder-free dishes that had been precoated with fetal calf serum (FCS) for 15 min in MEF (CF1 mice)-conditioned medium. EpiSC medium before MEF conditioning consisted of DMEM/F12 (Gibco BRL) containing 20% knockout (KO) serum replacement (Gibco BRL), 2 mM glutamine, 1× nonessential amino acids, and 5 ng/ml bFGF. For conditioning, irradiated MEFs were seeded at a density of 5×10^4 cells per square centimeter and incubated in EpiSC medium for 24 hr. The conditioned medium was filtered, and bFGF (5 ng/ml) was added (this was termed CM/FGF). EpiSCs were passaged using Accutase (Invitrogen) and seeded as single cells at approximately 15,000 cells per 6-cm dish. Medium was changed every 24 hr. ESCs, TR-GOF18, and TR/PD-converted cells were cultured on irradiated MEFs or on gelatin-coated plates in KO-DMEM medium containing 20% KO serum replacement, 2 mM glutamine, 1× nonessential amino acids, and LIF (1,000 U/ml). ESCs, TR-GOF18, and TR/PD-converted cells were passaged using trypsin (Invitrogen).

ESC Conversion of EpiSCs

EpiSCs were dissociated using Accutase and plated as single cells either on γ-irradiated MEF feeder cells or on FCS-coated tissue culture plates at low density (≤10,000 cells per well of a six-well plate) and cultured overnight in MEF-conditioned EpiSC medium supplemented with bFGF. Depending on

Figure 6. Epiblastin A/TR Treatment Simultaneously Activates WNT Signaling and Inhibits TGFbeta/SMAD2 Signaling

(A) Western blot analysis showing the effects of Epiblastin A and Chiron on BCATENIN, SMAD2, STAT3, and ERK phosphorylation in EpiSCs. The cells were treated with either Epiblastin A or Chiron for 30 min. An additional experiment was performed using a BCATENIN KO cell line to prove specific binding to p-BCATENIN of the applied antibody (lower band indicated with an arrow).

(B) Luciferase assay of TCF/Lef-mediated transcriptional activity in EpiSCs as a result of Epiblastin A and Chiron treatment. The Chiron was used as a positive control. The columns depict the TOP/FOP ratio (the data represent mean ± SD of triplicates; n = 3; and $p < 0.001$).

(C) Phenotypes of zebrafish embryos at 48 hpf. The embryos were allowed to grow in the presence of the indicated inhibitors from 7 hpf (the scale bar represents 500 μm).

(D) Clonal assay of Bcatenin$^{fl/fl}$ and Bcatenin$^{-/-}$ ESCs in the indicated culture conditions. Bcatenin$^{fl/fl}$ ESCs were plated at clonal density (600 cells) onto gelatin-coated plates and cultured for 7 days, after which, the cells were stained for AP and counted. To generate Bcatenin$^{-/-}$, Bcatenin$^{fl/fl}$ were plated as described earlier. After 48 hr, the cells were treated with 1 μM of 4-hydroxytamoxifen for 24 hr to induce the Cre excision of the floxed-Bcatenin. Western blot analysis demonstrates successful excision of Bcatenin after treatment with 4-hydroxytamoxifen (P, PD; C, CH; L, LIF; and E, Epiblastin A).

(E) Morphology and Oct4-GFP expression in sorted Oct4-GFP-negative E3 EpiSCs treated for 6 days with the indicated inhibitors as measured by FACS (the scale bar represents 200 μm).

(F) Real-time qPCR analysis of ICM marker gene expression in SB/CH-treated cells, EpiSCs, and ESCs. The gene expression levels are normalized to those of unsorted E3 EpiSC samples (the data represent mean ± SD of triplicates; n = 3).

(G) Schematic model of the mechanism by which TR/Epiblastin A reverts recalcitrant EpiSCs into ESCs. See text for discussion.

See also Figure S5.

the cell line, ROCK (Rho-associated protein kinase) inhibitor could be used to ensure higher cell survival after single-cell dissociation with Accutase. The next day, the EpiSC medium was replaced by the conversion medium. If not otherwise indicated, the conversion medium consisted of MEF-conditioned EpiSC medium containing 2 μM TR or Epiblastin A without additional bFGF. Higher concentrations of the compounds (>5 μM) were cytotoxic and increased cell death during conversion. The cells were cultured in the conversion medium for 8 days, and after the first 3 days, the medium was changed daily. OCT4-GFP-positive colonies usually started to appear on day 6. On day 8, the cells were dissociated with trypsin and replated at low density on MEF feeder cells or on a gelatin-coated cell culture dish in standard ESC medium supplemented with PD to allow for single-colony formation. For the first three to five passages, the newly formed ESC-like colonies were manually selected, dissociated with trypsin, and replated in a new culture dish.

Flow Cytometry

For fluorescence-activated cell sorting (FACS) and analysis, cell colonies were dissociated into single cells, as described earlier, resuspended in the corresponding culture medium at a cell density of approximately 5×10^6 cells per milliliter, and then analyzed using a FACSAria Cell Sorter (BD Biosciences).

Luciferase Assay

For quantifying relative *Oct4* enhancer activity, the PE and the DE were PCR amplified from a GOF18 plasmid (Yeom et al., 1996) and cloned into pGL3-Promoter (Promega). ESCs, EpiSCs, TR-GOF18, and TR/PD-converted cells were grown under feeder-free conditions and transfected using Lipofectamine 2000. All cells were seeded as single cells following Amaxa nucleofection (~2 million cells, 4 μg DNA, and program A-23) and assayed after 2 days. Values were normalized to the renilla and the empty vector signals.

Western Blot

Western blot analyses were performed following a standard procedure. Proteins were separated by SDS-PAGE and transferred onto nitrocellulose membranes. The membranes were incubated with the antibodies raised against phospho-S33/S37/T41-BCATENIN (Cell Signaling Technology [CST], #9561), phospho-S465/467-SMAD2 (CST, #3101), SMAD2/3 (CST, #3102), p-ERK (CST, #4370), ERK (CST, #9102), BCATENIN (BD Biosciences, C19220-050), phospho-STAT3 (Santa Cruz Biotechnology, sc-8059), and STAT3 (Santa Cruz, sc-482). Protein bands were visualized using ECL Prime Western Blotting Detection Reagent (GE Healthcare).

SUPPLEMENTAL INFORMATION

Supplemental Information includes five figures and one table and can be found with this article online at http://dx.doi.org/10.1016/j.celrep.2016.03.073.

AUTHOR CONTRIBUTIONS

Conceptualization, D.J.I., M.Z., and H.R.S.; Validation, J.C., B.G., D.C., I.C., and S.G.; Formal Analysis, M.J.A.-B.; Investigation, D.J.I., M.Z., A.U., R.O., K.-P.K., J.Y., G.W., D.E., D.S., K.S.G., S.H., and W.H.; Writing – Original Draft, D.J.I., M.Z., and H.R.S.; Writing – Review & Editing, D.J.I., M.Z., and H.R.S.; Visualization, D.J.I.; Supervision, S.Z., H.W., and H.R.S.; Funding Acquisition, H.W. and H.R.S.

ACKNOWLEDGMENTS

We are grateful to all members of the H.R.S. laboratory for fruitful discussions on the results. We are especially thankful to Dr. Austin Smith for providing the STAT3 KO ESCs and to Dr. Christof Bernemann for the EpiSC lines. Our special thanks go also to Dr. Dong Han and Sergiy Velychko for independent replication of the conversion experiments. We also thank Areti Malapetsas for final editing and Dr. Jeanine Müller-Keuker for assistance in figure formatting. We would like to thank Martina Sinn, Bärbel Schäfer, and David Obridge for technical assistance and Martin Stehling for FACS analyses. A.U. was supported by the IMPRS-CMB graduate school. K.S.G. and W.H. were supported by the NRW "return fellowship." This work was supported by the Max Planck Society.

Received: July 31, 2014
Revised: March 3, 2016
Accepted: March 18, 2016
Published: April 14, 2016

REFERENCES

Amit, S., Hatzubai, A., Birman, Y., Andersen, J.S., Ben-Shushan, E., Mann, M., Ben-Neriah, Y., and Alkalay, I. (2002). Axin-mediated CKI phosphorylation of beta-catenin at Ser 45: a molecular switch for the Wnt pathway. Genes Dev. *16*, 1066–1076.

Bao, S., Tang, F., Li, X., Hayashi, K., Gillich, A., Lao, K., and Surani, M.A. (2009). Epigenetic reversion of post-implantation epiblast to pluripotent embryonic stem cells. Nature *461*, 1292–1295.

Bernemann, C., Greber, B., Ko, K., Sterneckert, J., Han, D.W., Araúzo-Bravo, M.J., and Schöler, H.R. (2011). Distinct developmental ground states of epiblast stem cell lines determine different pluripotency features. Stem Cells *29*, 1496–1503.

Boroviak, T., Loos, R., Bertone, P., Smith, A., and Nichols, J. (2014). The ability of inner-cell-mass cells to self-renew as embryonic stem cells is acquired following epiblast specification. Nat. Cell Biol. *16*, 516–528.

Brault, V., Moore, R., Kutsch, S., Ishibashi, M., Rowitch, D.H., McMahon, A.P., Sommer, L., Boussadia, O., and Kemler, R. (2001). Inactivation of the beta-catenin gene by Wnt1-Cre-mediated deletion results in dramatic brain malformation and failure of craniofacial development. Development *128*, 1253–1264.

Brons, I.G., Smithers, L.E., Trotter, M.W., Rugg-Gunn, P., Sun, B., Chuva de Sousa Lopes, S.M., Howlett, S.K., Clarkson, A., Ahrlund-Richter, L., Pedersen, R.A., and Vallier, L. (2007). Derivation of pluripotent epiblast stem cells from mammalian embryos. Nature *448*, 191–195.

Chambers, I., Silva, J., Colby, D., Nichols, J., Nijmeijer, B., Robertson, M., Vrana, J., Jones, K., Grotewold, L., and Smith, A. (2007). Nanog safeguards pluripotency and mediates germline development. Nature *450*, 1230–1234.

Chou, Y.F., Chen, H.H., Eijpe, M., Yabuuchi, A., Chenoweth, J.G., Tesar, P., Lu, J., McKay, R.D., and Geijsen, N. (2008). The growth factor environment defines distinct pluripotent ground states in novel blastocyst-derived stem cells. Cell *135*, 449–461.

Corcino, J., Waxman, S., and Herbert, V. (1970). Mechanism of triamterene-induced megaloblastosis. Ann. Intern. Med. *73*, 419–424.

Dodsworth, B.T., Flynn, R., and Cowley, S.A. (2015). The current state of naïve human pluripotency. Stem Cells *33*, 3181–3186.

Dupre-Crochet, S., Figueroa, A., Hogan, C., Ferber, E.C., Bialucha, C.U., Adams, J., Richardson, E.C., and Fujita, Y. (2007). Casein kinase 1 is a novel negative regulator of E-cadherin-based cell-cell contacts. Mol. Cell. Biol. *27*, 3804–3816.

Evans, M.J., and Kaufman, M.H. (1981). Establishment in culture of pluripotential cells from mouse embryos. Nature *292*, 154–156.

Festuccia, N., Osorno, R., Halbritter, F., Karwacki-Neisius, V., Navarro, P., Colby, D., Wong, F., Yates, A., Tomlinson, S.R., and Chambers, I. (2012). Esrrb is a direct Nanog target gene that can substitute for Nanog function in pluripotent cells. Cell Stem Cell *11*, 477–490.

Gillich, A., Bao, S., Grabole, N., Hayashi, K., Trotter, M.W., Pasque, V., Magnúsdóttir, E., and Surani, M.A. (2012). Epiblast stem cell-based system reveals reprogramming synergy of germline factors. Cell Stem Cell *10*, 425–439.

Greber, B., Wu, G., Bernemann, C., Joo, J.Y., Han, D.W., Ko, K., Tapia, N., Sabour, D., Sterneckert, J., Tesar, P., and Schöler, H.R. (2010). Conserved and divergent roles of FGF signaling in mouse epiblast stem cells and human embryonic stem cells. Cell Stem Cell *6*, 215–226.

Guo, G., and Smith, A. (2010). A genome-wide screen in EpiSCs identifies Nr5a nuclear receptors as potent inducers of ground state pluripotency. Development *137*, 3185–3192.

Guo, G., Yang, J., Nichols, J., Hall, J.S., Eyres, I., Mansfield, W., and Smith, A. (2009). Klf4 reverts developmentally programmed restriction of ground state pluripotency. Development *136*, 1063–1069.

Hadjantonakis, A.K., Gertsenstein, M., Ikawa, M., Okabe, M., and Nagy, A. (1998). Non-invasive sexing of preimplantation stage mammalian embryos. Nat. Genet. *19*, 220–222.

Hall, J., Guo, G., Wray, J., Eyres, I., Nichols, J., Grotewold, L., Morfopoulou, S., Humphreys, P., Mansfield, W., Walker, R., et al. (2009). Oct4 and LIF/Stat3 additively induce Krüppel factors to sustain embryonic stem cell self-renewal. Cell Stem Cell *5*, 597–609.

Han, D.W., Tapia, N., Joo, J.Y., Greber, B., Araúzo-Bravo, M.J., Bernemann, C., Ko, K., Wu, G., Stehling, M., Do, J.T., and Schöler, H.R. (2010). Epiblast stem cell subpopulations represent mouse embryos of distinct pregastrulation stages. Cell *143*, 617–627.

Han, D.W., Greber, B., Wu, G., Tapia, N., Araúzo-Bravo, M.J., Ko, K., Bernemann, C., Stehling, M., and Schöler, H.R. (2011). Direct reprogramming of fibroblasts into epiblast stem cells. Nat. Cell Biol. *13*, 66–71.

Hanna, J., Markoulaki, S., Mitalipova, M., Cheng, A.W., Cassady, J.P., Staerk, J., Carey, B.W., Lengner, C.J., Foreman, R., Love, J., et al. (2009). Metastable pluripotent states in NOD-mouse-derived ESCs. Cell Stem Cell *4*, 513–524.

Hayashi, K., and Surani, M.A. (2009). Self-renewing epiblast stem cells exhibit continual delineation of germ cells with epigenetic reprogramming in vitro. Development *136*, 3549–3556.

Huang, Y., Osorno, R., Tsakiridis, A., and Wilson, V. (2012). In vivo differentiation potential of epiblast stem cells revealed by chimeric embryo formation. Cell Rep. *2*, 1571–1578.

Ichida, J.K., Blanchard, J., Lam, K., Son, E.Y., Chung, J.E., Egli, D., Loh, K.M., Carter, A.C., Di Giorgio, F.P., Koszka, K., et al. (2009). A small-molecule inhibitor of tgf-Beta signaling replaces sox2 in reprogramming by inducing nanog. Cell Stem Cell *5*, 491–503.

Karwacki-Neisius, V., Göke, J., Osorno, R., Halbritter, F., Ng, J.H., Weiße, A.Y., Wong, F.C., Gagliardi, A., Mullin, N.P., Festuccia, N., et al. (2013). Reduced Oct4 expression directs a robust pluripotent state with distinct signaling activity and increased enhancer occupancy by Oct4 and Nanog. Cell Stem Cell *12*, 531–545.

Kelly, K.F., Ng, D.Y., Jayakumaran, G., Wood, G.A., Koide, H., and Doble, B.W. (2011). β-catenin enhances Oct-4 activity and reinforces pluripotency through a TCF-independent mechanism. Cell Stem Cell *8*, 214–227.

Knippschild, U., Milne, D.M., Campbell, L.E., DeMaggio, A.J., Christenson, E., Hoekstra, M.F., and Meek, D.W. (1997). p53 is phosphorylated in vitro and in vivo by the delta and epsilon isoforms of casein kinase 1 and enhances the level of casein kinase 1 delta in response to topoisomerase-directed drugs. Oncogene *15*, 1727–1736.

Kunath, T., Saba-El-Leil, M.K., Almousailleakh, M., Wray, J., Meloche, S., and Smith, A. (2007). FGF stimulation of the Erk1/2 signalling cascade triggers transition of pluripotent embryonic stem cells from self-renewal to lineage commitment. Development *134*, 2895–2902.

Li, Z., and Rana, T.M. (2012). A kinase inhibitor screen identifies small-molecule enhancers of reprogramming and iPS cell generation. Nat. Commun. *3*, 1085.

Liu, C., Li, Y., Semenov, M., Han, C., Baeg, G.H., Tan, Y., Zhang, Z., Lin, X., and He, X. (2002). Control of beta-catenin phosphorylation/degradation by a dual-kinase mechanism. Cell *108*, 837–847.

Maherali, N., and Hochedlinger, K. (2009). Tgfbeta signal inhibition cooperates in the induction of iPSCs and replaces Sox2 and cMyc. Curr. Biol. *19*, 1718–1723.

Martin, G.R. (1981). Isolation of a pluripotent cell line from early mouse embryos cultured in medium conditioned by teratocarcinoma stem cells. Proc. Natl. Acad. Sci. USA *78*, 7634–7638.

Nie, B., Wang, H., Laurent, T., and Ding, S. (2012). Cellular reprogramming: a small molecule perspective. Curr. Opin. Cell Biol. *24*, 784–792.

Price, M.A. (2006). CKI, there's more than one: casein kinase I family members in Wnt and Hedgehog signaling. Genes Dev. *20*, 399–410.

Rena, G., Bain, J., Elliott, M., and Cohen, P. (2004). D4476, a cell-permeant inhibitor of CK1, suppresses the site-specific phosphorylation and nuclear exclusion of FOXO1a. EMBO Rep. *5*, 60–65.

Rubinfeld, B., Tice, D.A., and Polakis, P. (2001). Axin-dependent phosphorylation of the adenomatous polyposis coli protein mediated by casein kinase 1epsilon. J. Biol. Chem. *276*, 39037–39045.

Sato, N., Meijer, L., Skaltsounis, L., Greengard, P., and Brivanlou, A.H. (2004). Maintenance of pluripotency in human and mouse embryonic stem cells through activation of Wnt signaling by a pharmacological GSK-3-specific inhibitor. Nat. Med. *10*, 55–63.

Schalhorn, A., Siegert, W., and Sauer, H.J. (1981). Antifolate effect of triamterene on human leucocytes and on a human lymphoma cell line. Eur. J. Clin. Pharmacol. *20*, 219–224.

Silva, J., Nichols, J., Theunissen, T.W., Guo, G., van Oosten, A.L., Barrandon, O., Wray, J., Yamanaka, S., Chambers, I., and Smith, A. (2009). Nanog is the gateway to the pluripotent ground state. Cell *138*, 722–737.

Swiatek, W., Kang, H., Garcia, B.A., Shabanowitz, J., Coombs, G.S., Hunt, D.F., and Virshup, D.M. (2006). Negative regulation of LRP6 function by casein kinase I epsilon phosphorylation. J. Biol. Chem. *281*, 12233–12241.

Tai, C.I., and Ying, Q.L. (2013). Gbx2, a LIF/Stat3 target, promotes reprogramming to and retention of the pluripotent ground state. J. Cell Sci. *126*, 1093–1098.

ten Berge, D., Kurek, D., Blauwkamp, T., Koole, W., Maas, A., Eroglu, E., Siu, R.K., and Nusse, R. (2011). Embryonic stem cells require Wnt proteins to prevent differentiation to epiblast stem cells. Nat. Cell Biol. *13*, 1070–1075.

Tesar, P.J., Chenoweth, J.G., Brook, F.A., Davies, T.J., Evans, E.P., Mack, D.L., Gardner, R.L., and McKay, R.D. (2007). New cell lines from mouse epiblast share defining features with human embryonic stem cells. Nature *448*, 196–199.

Tsakiridis, A., Huang, Y., Blin, G., Skylaki, S., Wymeersch, F., Osorno, R., Economou, C., Karagianni, E., Zhao, S., Lowell, S., and Wilson, V. (2014). Distinct Wnt-driven primitive streak-like populations reflect in vivo lineage precursors. Development *141*, 1209–1221.

Ursu, A., Illich, D.J., Takemoto, Y., Porfetye, A.T., Zhang, M., Brockmeyer, A., Janning, P., Watanabe, N., Osada, H., Vetter, I.R., et al. (2016). Epiblastin A induces reprogramming of epiblast stem cells into embryonic stem cells by inhibition of casein kinase 1. Cell Chem. Biol. Published online March 31, 2016. http://dx.doi.org/10.1016/j.chembiol.2016.02.015.

Waddell, D.S., Liberati, N.T., Guo, X., Frederick, J.P., and Wang, X.F. (2004). Casein kinase Iepsilon plays a functional role in the transforming growth factor-beta signaling pathway. J. Biol. Chem. *279*, 29236–29246.

Ware, C.B., Wang, L., Mecham, B.H., Shen, L., Nelson, A.M., Bar, M., Lamba, D.A., Dauphin, D.S., Buckingham, B., Askari, B., et al. (2009). Histone deacetylase inhibition elicits an evolutionarily conserved self-renewal program in embryonic stem cells. Cell Stem Cell *4*, 359–369.

Wray, J., Kalkan, T., Gomez-Lopez, S., Eckardt, D., Cook, A., Kemler, R., and Smith, A. (2011). Inhibition of glycogen synthase kinase-3 alleviates Tcf3 repression of the pluripotency network and increases embryonic stem cell resistance to differentiation. Nat. Cell Biol. *13*, 838–845.

Yeom, Y.I., Fuhrmann, G., Ovitt, C.E., Brehm, A., Ohbo, K., Gross, M., Hübner, K., and Schöler, H.R. (1996). Germline regulatory element of Oct-4 specific for the totipotent cycle of embryonal cells. Development *122*, 881–894.

Ying, Q.L., Wray, J., Nichols, J., Batlle-Morera, L., Doble, B., Woodgett, J., Cohen, P., and Smith, A. (2008). The ground state of embryonic stem cell self-renewal. Nature *453*, 519–523.

Zhou, H., Li, W., Zhu, S., Joo, J.Y., Do, J.T., Xiong, W., Kim, J.B., Zhang, K., Schöler, H.R., and Ding, S. (2010). Conversion of mouse epiblast stem cells to an earlier pluripotency state by small molecules. J. Biol. Chem. *285*, 29676–29680.